

Thermal process dependence of Li configuration and electrical properties of Li-doped ZnO

Z. Zhang, , K. E. Knutsen, , T. Merz, , A. Yu. Kuznetsov, , B. G. Svensson, and , and L. J. Brillson

Citation: *Appl. Phys. Lett.* **100**, 042107 (2012); doi: 10.1063/1.3679708

View online: <http://dx.doi.org/10.1063/1.3679708>

View Table of Contents: <http://aip.scitation.org/toc/apl/100/4>

Published by the [American Institute of Physics](#)

Articles you may be interested in

[Control of *p*- and *n*-type conductivities in Li-doped ZnO thin films](#)

Applied Physics Letters **89**, 112113 (2006); 10.1063/1.2354034

[Investigation on the formation mechanism of *p*-type Li-N dual-doped ZnO](#)

Applied Physics Letters **97**, 222101 (2010); 10.1063/1.3518059



The advertisement features a stylized circuit board background with various components and labels. The labels include 'COMPUTING', 'ENGINEERING', and 'SCIENCE'. A small image of the magazine cover is shown in the bottom right corner, with the title 'Computing' and the subtitle 'SCIENCE ENGINEERING'. The cover also features the text 'EXPLORING OUR SOLAR SYSTEM' and an illustration of a rocket launching into space.

CiSE magazine is an innovative blend.

Thermal process dependence of Li configuration and electrical properties of Li-doped ZnO

Z. Zhang,^{1,a)} K. E. Knutsen,² T. Merz,³ A. Yu. Kuznetsov,² B. G. Svensson,³ and L. J. Brillson^{1,3,4}

¹*Department of Electrical and Computer Engineering, The Ohio State University, Columbus, Ohio 43210, USA*

²*Department of Physics, University of Oslo, P.O. Box 1048 Blindern, N-0316 Oslo, Norway*

³*Department of Physics, The Ohio State University, Columbus, Ohio 43210, USA*

⁴*Center for Materials Research, The Ohio State University, Columbus, Ohio 43210, USA*

(Received 29 July 2011; accepted 7 January 2012; published online 26 January 2012)

We used depth-resolved cathodoluminescence spectroscopy (DRCLS) to describe the strong dependence of Li acceptor formation on thermal treatment in Li-doped ZnO. Within a 500-600 °C annealing temperature range, subsequent quenching ZnO leaves Li as interstitial donors, resulting in low room temperature resistivity, while slow cooling in air allows these interstitials to fill Zn vacancies forming Li acceptors 3.0 eV below the conduction band edge. DRCLS reveals an inverse relationship between the optical emission densities of lithium on zinc sites versus zinc vacancy sites, demonstrating the time dependence of Li interstitials to combine with zinc vacancies in order to form substitutional Li acceptors. © 2012 American Institute of Physics. [doi:10.1063/1.3679708]

The wide band gap semiconductor ZnO is a leading candidate for next generation opto- and microelectronics due to its high exciton binding energy, thermochemical stability, environmental compatibility, and potential applications for light emitting devices and photovoltaics.^{1,2} However, the ability to controllably dope ZnO p-type remains a fundamental, unresolved challenge. Efforts include attempts to control the amphoteric electrical behavior of Li in ZnO.^{3,4} Li is unintentionally incorporated in hydrothermal (HT)-ZnO during synthesis or intentionally added during growth or implanted afterwards. Calculations suggest Li interstitials (Li_i) are donors but shallow acceptors on zinc sites (Li_{Zn}).³⁻⁶ However, HT-ZnO wafers and Li-doped ZnO are usually highly resistive due to self-compensation and the low energy barrier for Li to switch between interstitial and substitutional sites.^{3,4}

Previously it has been shown that Li concentration and electrical properties can be manipulated by vacancy cluster gettering or high temperature treatments.^{3,7} Combined depth-resolved cathodoluminescence spectroscopy (DRCLS), positron annihilation spectroscopy (PAS), and surface photovoltage spectroscopy (SPS) of Li-implanted HT-ZnO have correlated the commonly observed 1.9-2.1 eV “red” and 2.3-2.5 eV “green” luminescence with zinc vacancy (V_{Zn}) and vacancy clusters and oxygen vacancy (V_{O})-related defects, respectively.⁸ Secondary ion mass spectrometry (SIMS) and deep level transient spectroscopy (DLTS) suggest that Li atoms in HT-ZnO act almost exclusively as substitutional acceptors (Li_{Zn}) that compensate donors for Fermi levels above mid-gap.⁹ However, resistivities are strongly dependent on annealing, and the energy level position of Li_{Zn} acceptors and Li configurations under different treatment are still undetermined. Here, we show that Li configuration can be monitored by DRCLS and controlled following 500-600 °C annealing by cooling rate to obtain either Li_{Zn} or Li_i configurations in Li doped ZnO.

We studied both Li-doped melt-grown (MG)-ZnO from Cermet Inc. and HT-ZnO from SPC Goodwill with different

temperature anneals and cooling rates. The as-grown MG-ZnO had very low Li background concentration, 10^{15} - 10^{16} Li atoms per cm^3 , n-type, and low resistivity ($\sim 1.2 \Omega \text{ cm}$). They were annealed 10 min in 5% Li_2O and ZnO powder at various temperatures from 500 °C to 600 °C, with some quenched in DI water and the others slow-cooled in air. All as-grown HT-ZnO were unintentionally doped with $1-5 \times 10^{17}$ Li atoms per cm^3 with some annealed in 10% Li_2O and ZnO powder for 1 h then either: (i) quenched in DI H_2O or (ii) annealed in air at 600 °C for an additional 10 min with slow cooling in air. Both annealing processes avoid any Zn interstitial formation that could occur under Zn-rich atmosphere annealing.¹⁰ DRCLS measurements were obtained on ZnO(000-1) faces at 80 K in ultrahigh vacuum using the method described in Refs. 11 and 12. Monte Carlo simulation¹³ provides depth distributions of the electron-hole pairs generated by the incident electron beam versus the beam energy (E_B). For incident energy $E_B = 1, 2, 3, 4,$ and 5 keV, electron-hole pair excitation peaks at $U_0 = 7, 18, 32, 50,$ and 72 nm, respectively.

Figure 1 shows DRCLS spectra of MG-ZnO samples after 500 °C anneal and different cooling methods. Emission intensities due to V_{Zn} - and V_{O} -related native defects in as-grown MG-ZnO are orders-of-magnitude lower than the dominant near band edge (NBE) 3.39 eV peak. Figure 1(a) shows that, after annealing in Li_2O and ZnO powder and quenching, MG-ZnO emission at 2.07 eV associated with V_{Zn} clusters increases by nearly three orders of magnitude.⁸ The annealed and slow-cooled MG-ZnO also displays this deep level defect increase but, in contrast, it clearly shows an additional feature at 3.0 eV. Figure 1(a) illustrates the uniformity of this difference at all depths and Figure 1(b) compares this contrast for $E_B = 5$ keV. Furthermore, the 2.07 eV feature is lower in the slow-cooled MG-ZnO. Four-point probe measurement showed that the quenched sample had low resistivity, $0.94 \Omega \text{ cm}$, while the slow-cooled MG-ZnO was semi-insulating.

As reported by recent theory calculations and experiments,¹⁴⁻¹⁸ the concentration of intrinsic defects

^{a)}Electronic mail: zhang.720@osu.edu.

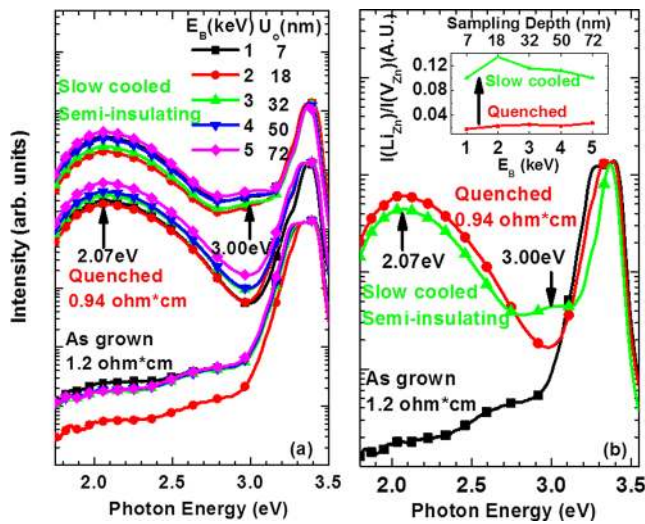


FIG. 1. (Color online) 80 K CL spectra for Li-doped MG-ZnO (a) as-grown, annealed in 500°C and quenched in DI water or slow cooled in air and (b) 5 keV CL spectra comparison and (inset) relative intensity changes of V_{Zn} and Li_{Zn} related defects in MG-ZnO after quenching and slow cooling process. The slow-cooled MG-ZnO exhibits an additional 3.0 eV peak.

depends strongly on the Fermi-level position (E_F), and in our samples E_F is in the upper half of the bandgap, typically less than 0.3 eV below E_C . The formation energy of zinc interstitial (Zn_i) is so high that the concentration of Zn_i is orders of magnitude smaller than V_{Zn} in our samples¹⁴ and Zn_i can be ignored. Also the formation energy of interstitial oxygen (O_i) is substantially higher than that of V_{Zn} in our samples¹⁴ and so O_i can be ignored. V_O can exist in our samples with significant concentration, but here we have the identification of V_O with the 2.5 eV CL-peak⁸ and previous literature.¹⁹ Furthermore, V_O is a double donor center with its energy level located about 0.6-0.8 eV below E_C .^{8,14-18} Therefore, V_O has nothing directly to do with the 3.0 eV CL peak. This indicates that Li diffuses into the MG-ZnO during the 500°C anneal, and acts as an ionized interstitial Li donor at room temperature. This is consistent with theory of low activation energy for Li diffusion.²⁰ For the quenched MG-ZnO, the interstitial Li has insufficient time to diffuse to substitutional sites, remaining as a donor during this fast (~ 1 s) cooling process and accounting for the low four-point probe resistivity. During the slow cooling process in air ($\sim 1.5 \pm 0.5$ min), however, the Li_i donor has time to diffuse and fill in V_{Zn} sites and become substitutional Li_{Zn} , increasing resistivity by compensating Li_i and other intrinsic (V_O)¹⁵ and extrinsic donors.²¹⁻²³

Scanning spreading resistivity measurement (SSRM) profiles of Li-doped MG-ZnO in Figure 2(a) confirm this resistivity difference between quenched and slow-cooled specimens. The slow-cooled MG-ZnO has eight orders of magnitude higher resistivity than the quenched MG-ZnO. Figure 2(b) shows that quenched and slow-cooled MG-ZnO after 500°C annealing have similar Li profiles, demonstrating that resistivity changes were not due to Li concentration differences but rather to changes in Li lattice configuration. Figures 2(a) and 2(b) also show the direct correspondence in depth and relative magnitude between slow-cooled Li SSRM and SIMS profiles at both 525°C and 550°C, indicating that the slow-cooled Li acts as an acceptor, compensating the otherwise n-type back-

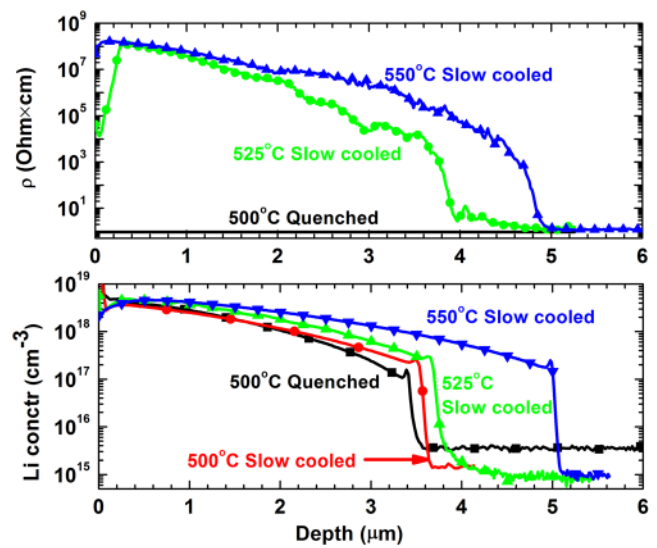


FIG. 2. (Color online) (a) SSRM of slow cooled MG-ZnO samples after 500°C–550°C annealing showing contrast between quenched and slow-cooled methods. (b) SIMS of quenched and slow-cooled MG-ZnO after 500–550°C annealing showing correspondence between Li density and resistivity in slow-cooled samples.

ground doping. Indeed, PAS shows that slow cooling in these samples results in formation of Li_{Zn} acceptors with high density, larger than $2-3 \times 10^{18} \text{ cm}^{-3}$, while the V_{Zn} concentration is on the order of $5 \times 10^{16} \text{ cm}^{-3}$.²⁴

Figure 3 illustrates the depth dependence of the 3.0 eV feature and its correspondence with the SIMS Li profile in slow cooled MG-ZnO. Both the 3.0 eV DRCLS intensity and the SIMS Li concentration increase with depth over the same nanometer scale. The inset shows that the 3.0 eV peak intensity ($I(Li_{Zn})/I(NBE)$) increases from 32 nm to above 72 nm, while its SIMS profile [Li] increases from the surface to

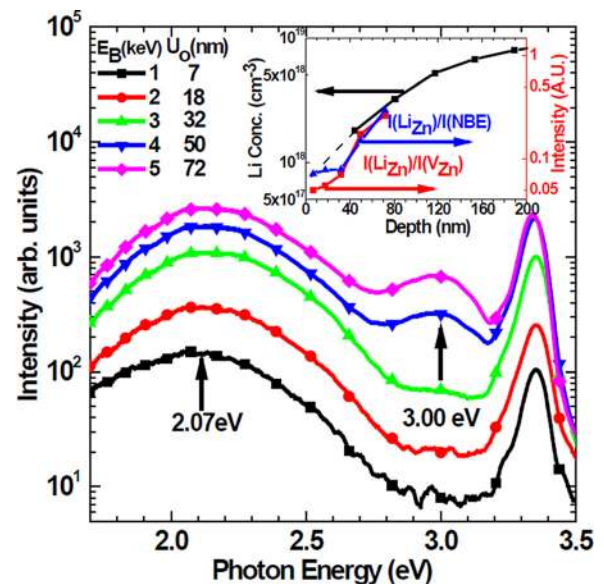


FIG. 3. (Color online) 80 K CL spectra for Li-doped MG-ZnO annealed at 600°C and slow cooled in air, and [Li] SIMS profile correspondence with Li_{Zn} versus V_{Zn} DRCLS intensities (inset). The 3.0 eV Li_{Zn} increases from 32 nm below the surface to above 72 nm, and corresponds to the [Li] profile in this range. The increasing (decreasing) Li_{Zn} (V_{Zn})-related intensities show that Li_{Zn} forms by Li filling V_{Zn} sites.

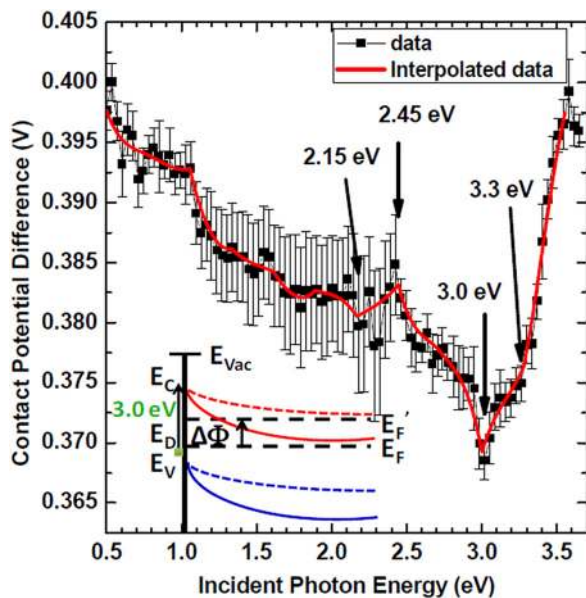


FIG. 4. (Color online) SPS spectrum of flash-annealed, slow-cooled Li-implanted HT-ZnO showing onset of photodepopulation from 3.0 eV acceptor state, decreased band bending, and higher Fermi level.

above 200 nm. The correspondence between DRCLS 3.0 eV emission and SIMS Li profile in Figure 3 coupled with the correspondence between the SIMS Li profile and resistivity increase due to Li_{Zn} acceptors in Figure 2 suggest strongly that the 3.0 eV feature is characteristic of Li_{Zn} acceptor. Figure 3 also reveals an interplay between the 2.07 eV V_{Zn} cluster feature and the 3.0 eV Li_{Zn} peak. As the Li_{Zn} intensity increases with depth, the V_{Zn} -related feature decreases so that their ratio increases with depth. The movement of Li from interstitial to Zn substitutional sites decreases the 2.07 eV (V_{Zn} -related) peak intensity and increases 3.0 eV (Li_{Zn} -related), increasing the intensity ratio $I(\text{Li}_{\text{Zn}})/I(\text{V}_{\text{Zn}})$, as the Figure 3 inset illustrates.

HT-ZnO specimens after quenching and slow cooling display the same physical behavior as MG-ZnO samples: (i) a new 3.0 eV DRCLS peak in slow-cooled, semi-insulating HT-ZnO, (ii) a systematic decrease of the 2.07 eV V_{Zn} -related peak intensity with increasing 3.0 eV intensity, and (iii) the absence of the 3.0 eV peak for the quenched, low resistivity HT-ZnO. Again, the 3.0 eV peak, follows the Li concentration on a nanometer scale. From the SIMS-DRCLS comparison, the lower detection limit of the 3.0 eV Li_{Zn} peak is found to be $\sim 5 \times 10^{17} \text{ cm}^{-3}$.

Previous studies of thermally processed Li-implanted ZnO at micron depths support these results. Flash annealed (20 ms at 1200 °C) from a 500 °C baseline and slow cooled Li-implanted HT-ZnO shows a 3.0 eV peak emerging at 950 nm and its intensity peaking at 1.5 μm depth,⁸ corresponding to the peak SIMS [Li] concentration at the same depth.⁷ Optical studies are consistent with the assignment of the 3.0 eV peak to Li_{Zn} dopant sites. SPS of these slow-cooled MG- and HT-ZnO specimens in Figure 4 display features corresponding to optical depopulation of states 3.0 eV below the conduction band edge (E_{C}).²⁵ The $E_{\text{C}} - 3.0 \text{ eV}$ energy assignment is consistent with theoretical predictions by Lany and Zunger²⁶ and with photoluminescence (PL) results of Li dif-

fused ZnO by Meyer *et al.*^{27,28} Early diffusion studies highlighted the possible interplay between interstitial Li and Li_{Zn} .^{28,29} Our results demonstrate this interplay explicitly and the pivotal role of thermal treatment in controlling the balance of Li donors and acceptors.

In summary, we have used several depth-resolved techniques to identify the 3.0 eV luminescence peak in Li-doped ZnO with Li on Zn acceptor states located 0.3 eV above the valence band. The evolution of Li configurations in ZnO from interstitial donor to substitutional acceptor under different annealing conditions emphasizes the sensitive temperature balance required to diffuse interstitial Li into Zn vacancy sites to promote acceptor doping.

The authors gratefully acknowledge support from the National Science Foundation Grant No. DMR-0803276 (Charles Ying), ECCS-0923805, and the Norwegian Research Council NANOMAT program.

- ¹D. C. Look, *Mater. Sci. Eng. B* **80**, 383 (2001).
- ²S. J. Pearton, D. P. Norton, L. Ip, Y. W. Heo, and T. Steiner, *Prog. Mater. Sci.* **50**, 293 (2005).
- ³E. V. Monakhov, A. Yu. Kuznetsov, and B. G. Svensson, *J. Phys. D* **42**, 153001 (2009).
- ⁴M. G. Wardle, J. P. Goss, and P. R. Briddon, *Phys. Rev. B* **71**, 155205 (2005).
- ⁵E.-C. Lee and K. J. Chang, *Phys. Rev. B* **70**, 115210 (2004).
- ⁶Y. J. Zeng, Z. Z. Ye, W. Z. Xu, D. Y. Li, J. G. Lu, L. P. Zhu, and B. H. Zhao, *Appl. Phys. Lett.* **88**, 062107 (2006).
- ⁷T. Moe Børseth, F. Tuomisto, J. S. Christensen, W. Skorupa, E. V. Monakhov, B. G. Svensson, and A. Yu. Kuznetsov, *Phys. Rev. B* **74**, 161202(R) (2006).
- ⁸Y. Dong, F. Tuomisto, B. G. Svensson, A. Yu. Kuznetsov, and L. J. Brillson, *Phys. Rev. B* **81**, 081201(R) (2010).
- ⁹L. Vines, E. V. Monakhov, R. Schifano, W. Mtangi, F. D. Auret, and B. G. Svensson, *J. Appl. Phys.* **107**, 103707 (2010).
- ¹⁰B. R. Appleton and L. C. Feldman, *J. Phys. Chem. Solids* **33**, 507 (1972).
- ¹¹L. J. Brillson, *J. Vac. Sci. Technol. B* **19**, 1762 (2001).
- ¹²E. J. Katz, Z. Zhang, H. L. Hughes, K.-B. Chung, G. Lucovsky, and L. J. Brillson, *J. Vac. Sci. Technol. B* **29**, 011027 (2011).
- ¹³D. Drouin, A. R. Couture, D. Joly, X. Tastet, V. Aimez, and R. Gauvin, *Scanning* **29**, 92 (2007).
- ¹⁴R. Vidya, P. Ravindran, H. Fjellvåg, B. G. Svensson, E. Monakhov, M. Ganchenkova, and R. M. Nieminen, *Phys. Rev. B* **83**, 045206 (2011).
- ¹⁵A. Janotti and C. G. Van de Walle, *Phys. Rev. B* **76**, 165202 (2007).
- ¹⁶F. A. Selim, M. H. Weber, D. Solodovnikov, and K. G. Lynn, *Phys. Rev. Lett.* **99**, 085502 (2007).
- ¹⁷M. D. McCluskey and S. J. Jokela, *J. Appl. Phys.* **106**, 071101 (2009).
- ¹⁸F. Oba, M. Choi, A. Togo, and S. Tanaka, *Sci. Technol. Adv. Mater.* **12**, 034302 (2011).
- ¹⁹K. Vanheusden, C. H. Seager, W. L. Warren, D. R. Tallant, and J. A. Voigt, *Appl. Phys. Lett.* **68**, 403 (1996).
- ²⁰A. Carvalho, A. Alkauskas, A. Pasquarello, A. K. Tagantsev, and N. Setter, *Phys. Rev. B* **80**, 195205 (2009).
- ²¹S. Zhang, S.-H. Wei, and A. Zunger, *Phys. Rev. B* **63**, 075205 (2001).
- ²²J. Hu and R. G. Gordon, *Mater. Res. Soc. Symp. Proc.* **283**, 891 (1993).
- ²³A. Janotti and C. G. Van de Walle, *Nature Mater.* **6**, 44 (2007).
- ²⁴K. M. Johansen, A. Zubiaga, I. Makkonen, F. Tuomisto, P. T. Neuvonen, K. E. Knutsen, E. V. Monakhov, A. Yu. Kuznetsov, and B. G. Svensson, *Phys. Rev. B* **83**, 245208 (2011).
- ²⁵Z. Zhang, K.-E. Knutsen, T. Merz, A. Yu. Kuznetsov, B. G. Svensson, and L. J. Brillson "Thermal process dependence of Li configuration and electronic properties in Li-doped ZnO," (unpublished).
- ²⁶S. Lany and A. Zunger, *Appl. Phys. Lett.* **96**, 142114 (2010).
- ²⁷B. K. Meyer, J. Sann, and A. Zeuner, *Superlattices Microstruct.* **38**, 344 (2005).
- ²⁸B. K. Meyer, J. Stehr, A. Hofstaetter, N. Volbers, A. Zeuner, and J. Sann, *Appl. Phys. A: Mater. Sci. Process.* **88**, 119 (2007).
- ²⁹J. J. Lander, *J. Phys. Chem. Solids* **15**, 324 (1960).